

Research Article

## Effectiveness of Cellulose-Based Co-Fe LDH Composite Synthetic Clay as an Eliminator of Sulfamethoxazole and Cefixime Residues: Evaluation of Green Metrics and Cytotoxicity

Ahmed A. Allam<sup>1,2</sup>, Asmaa M. Salah<sup>3</sup>, Amna A.Kotp<sup>4</sup>, Wesam kamal<sup>3</sup>, Doaa Essam<sup>5</sup>, Samar M. Mahgoub<sup>4</sup>, Mahmoud A. Mohamed<sup>6</sup>, Zienab E. Eldin<sup>4</sup>, Haifa E. Alfassam<sup>7</sup>, Hassan A. Rudayni<sup>1</sup>, Rehab Mahmoud<sup>8\*</sup>

<sup>1</sup> Department of Biology, College of Science, Imam Muhammad Ibn Saud Islamic University, Riyadh 11623, Saudi Arabia.

<sup>2</sup> Department of Zoology, Faculty of Science, Beni-suef University, Beni-suef 65211 Egypt.

<sup>3</sup> Chemistry Department, Faculty of Science, Beni-Suef University, Beni-Suef 62511, Egypt.

<sup>4</sup> Materials Science and Nanotechnology Department, Faculty of Postgraduate Studies for Advanced Science (PSAS), Beni-Suef University, Beni-Suef 62511, Egypt.

<sup>5</sup> Nanomaterials Science Research Laboratory, Chemistry Department, Faculty of Science, Beni-Suef University, Beni-Suef, Egypt.

<sup>6</sup> Hikma Pharmaceutical Company, Beni-Suef, Egypt.

<sup>7</sup> Department of Biology, college of Science, Princess Nourah bint Abdulrahman University, P.O. BOX 84428, Riyadh 11671, Saudi Arabia.

<sup>8</sup> Department of chemistry, faculty of science, Beni-Suef University, Egypt.

**\*Corresponding Author:** Rehab Mahmoud, Department of chemistry, faculty of science, Beni-Suef University, Egypt.

**Citation:** Ahmed A. Allam, Asmaa M. Salah, Amna A.Kotp, Wesam kamal, Rehab Mahmoud, et al. (2024) Effectiveness of Cellulose-Based Co-Fe LDH Composite Synthetic Clay as an Eliminator of Sulfamethoxazole and Cefixime Residues: Evaluation of Green Metrics and Cytotoxicity. *Nano Technol & Nano Sci J* 6: 157.

**Received:** May 19, 2024; **Accepted:** July 04, 2024; **Published:** July10, 2024.

**Copyright:** © 2024 Rehab Mahmoud, et al. This is an open-access article distributed under the terms of the Creative Commons Attribution License, which permits unrestricted use, distribution, and reproduction in any medium, provided the original author and source are credited.

### Abstract

The rise of antibiotic residues poses a serious threat to ecological and aquatic environments, necessitating the

development of cost-effective, convenient, and recyclable adsorbents. In our study, we used cellulose based layered double hydroxide (LDH) as an efficient adsorbent and nano-carrier for both Sulfamethoxazole (SMX); Cefixime (CFX) residues due to their biodegradability and biocompatibility. Chemical processes are measured according to green chemistry metrics to identify which features adhere to the principles. A GREENness Assessment (ESA), Analytical GREENness Preparation (AGREEprep), and Analytical Eco-Scale Assessments (ESA) were used to assess the suitability of the proposed analytical method. We extensively analyzed the synthesized Co-Fe LDH/Cellulose before and after the adsorption processes using XRD, FTIR, and SEM. We investigated the factors affecting the adsorption process, such as pH, adsorbent dose, Concentrations of Sulfamethoxazole and Cefixime and time. The residual concentrations of antibiotic residues were measured using a double beam UV–visible spectrophotometer (UV-2600 UV-Vis Spectrophotometer, Shimadzu) at wavelength 265 nm, 288 nm for Sulfamethoxazole (SMX); Cefixime (CFX) respectively. We studied six non-linear adsorption isotherm models at pH 5 using Co-Fe LDH showing maximum adsorption capacities ( $q_{max}$ ) of 272.13 mg/g for SMX and 208.00 mg/g for CFX. Kinetic studies were also conducted. The MTT assay was performed on vero cells in direct contact with LDHs nanocomposites to evaluate the cytotoxicity and side effects of Cellulose-based Co-Fe LDH. Cellulose-based Co-Fe LDH nanocomposite demonstrate excellent cytocompatibility and less cytotoxic effects on the tested cell line. These results validate the potential use of these unique LDH-based cellulose cytocompatible biomaterials for water treatment application.

**Keywords:** *Sulfamethoxazole; Cefixime; Cellulose-Based Co-Fe LDH; Adsorption; Waste Water*

## Introduction

Antibiotics are widely used in human medicine, veterinary medicine, and aquaculture to prevent or treat microbial infections [1,2]. Global human consumption of antibiotics has increased significantly and the release of antibiotics into the environment is a major concern due to the selection of antimicrobial resistance [3,4]. Over prescription and overuse of antibiotics is a problem in many hospitals, with rates of antibiotics prescription significantly higher than the world average [5]. Antibiotics pose the primary risk to soil and aquatic ecosystems, making them the focus of the present study [6]. It is important to note that pharmaceutical residues are often found in combination in water, which can lead to potential toxic interactions. Sulfamethoxazole (SMX), a common antibiotic used in livestock and human treatment, is frequently released into water through wastewater treatment plants and the use of manure from medicated animals and humans on agricultural land [7]. Moreover, CFX is poorly absorbed in the gastrointestinal system and possesses the potential to seriously harm aquatic environments owing to its low bioavailability. This antibiotic is applied to avoid infections in patients who have had significant surgery in addition to treating a variety of bacterial illnesses [8]. Water bodies emit and detect large amounts of CFX, a commonly given cephalosporin antibiotic, which causes accidental accumulation into aquatic organisms [9]. Sulfamethoxazole (SMX) and Cefixime (CFX) are considered to be highly hazardous antibiotics present in waste waters in different regions of the world with a risk quotient (RQ) that exceeds 1. Due to its high water-solubility, SMX is often found in surface water, groundwater, and drinking water [10], and can accumulate and spread in the environment, impacting the biosphere [11]. Conventional biological treatments in municipal wastewater treatment plants have difficulty removing SMX [12,13], highlighting the need for innovative technologies for SMX removal. Exposure to both SMX and microplastics has been found to exacerbate growth toxicity in zebrafish and the nematode *Caenorhabditis elegans*, indicating a synergistic effect [14].

Several studies have been reported on the removal of Sulfamethoxazole from wastewater including conventional treatment methods such as activated sludge and membrane bioreactors can remove some Sulfamethoxazole from wastewater. However, small amounts may still remain in the treated effluent, necessitating more advanced removal techniques. Prasannamedha et al have reported an enhanced adsorptive removal of SMX using biochar derived from sugarcane bagasse showing maximum adsorption capacity of 400 mg/g through spontaneous reaction [15]. Whereas, the adsorption capacity of SMX using large specific area of biochar derived from corncob xylose residue has recorded 1429 mg/g [16]. Niu et al used Na<sub>2</sub>CO<sub>3</sub>-modified biochar derived from sorghum straw and sewage sludge to remove SMX showing maximum adsorption capacity of 139.8 mg/g [17]. In addition to different removal techniques that were excluded due to their high cost and danger including conductive-diamond electrochemical oxidation [18]; ozonation. Since CFX is often used to treat a broad range of illnesses and their presence in solutions may be highly harmful, it is crucial to remove them from solutions before allowing them to enter the environment [19]. Many different methods have been reported to remove CFX from water including photocatalysis [20,21], membrane [22], photo-Fenton [23], biological [24], and adsorption [25-27]. Adsorption is superior to other techniques in a number of ways when it comes to removing dyes, heavy metals, and pharmaceuticals. These consist of low operating costs, high recovery, low adsorbent consumption, high efficiency, insensitivity to hazardous chemicals and pollutants, high adaptability, minimal formation of secondary materials in the system, and specific surface area for removal [28,29]. UDDIN et al. discovered that chitosan 10B has a maximum cefixime adsorption capacity of 37.04 μmol/g [30]. Emami et al. studied the adsorption of CFX on the HKUST-1/ZIF-8 nanocomposite synthesized using a facile and green ultrasonic and showed 110 mg/g as the greatest amount of adsorbed CFX [25]. Zadvarzi et al. verified the highest adsorption capacity for CFX to be 588 mg/g when the chitosan-polyacrylamide was produced by ZIF-8 to create chitosan@polyacrylamide@ZIF-8 [31]. Moridi et al. employed nZVI/CS to remove CFX from water-based solutions and got a maximum adsorption capacity of 4.31 mg/g [27]. Other studies reporting adsorbents for removal of CTX and SMX are summarized in Table 1.

Layered double hydroxides (LDHs) are well-known adsorbents with advantages such as large adsorption capacity and high economic viability. They can be easily fabricated into high-purity, well-crystalline nano composites using co-precipitation techniques. Cellulose is a natural biopolymer that is abundant, biodegradable, and renewable [36]. It has been utilized for removing pollutants from both aqueous and non-aqueous solutions [37]. Microcrystalline cellulose (MCC) is derived from dissolving pulp grade, a purified form of plant cellulose, and is known for its inert and stable nature, making it an effective emulsion and foam stabilizer [38]. MCC has been employed as a bio-template for producing LDH networks due to its non-toxic and renewable properties. It can prevent an increase in nanoparticle size, ensure reproducibility, and organize different functions and interfaces [39]. The use of bio-based templates like MCC for LDHs is a promising direction for future research, as they can be produced from inexpensive and abundant precursors using environmentally friendly methods and can be removed under mild conditions [40].

In this work, Co-Fe LDH/Cellulose was synthesized by incorporating Cellulose into the Co-Fe LDH structure of by the co-precipitation method. This adsorbent was subsequently employed to adsorb SMX and CFX. Furthermore, while analyzing the impact of effective factors on the adsorption process, Co-Fe LDH/Cellulose nanocomposite exhibited a significant performance. The physical characteristics of Co-Fe LDH/Cellulose was investigated using XRD, FTIR,

SEM, EDX, TGA, BET surface area and zeta characteristics. To determine the ideal parameters that affect several elements including pH, amount of adsorbent, starting concentration, temperature and contact time in adsorption process. Isotherm and kinetic models were studied in order to determine key equilibrium data and the rate of adsorption process respectively.

**Table 1:** Previous studies in the open literature reporting adsorbents for SFX and CFX removal.

Adsorbent	pH	Adsorbent mass (g/L)	Equilibrium time (min)	Removal percent%	q <sub>max</sub> (mg/g) for SFX	Ref
Co-Fe LDH/Cellulose	5	0.1	15	94	272.13	This work
Iron-activated bermudagrass-derived biochar	3	0.01	10	97	253	[32]
Surface imprinted polymer on a metal-organic framework	8	-	10	-	284.66	[33]
Ag <sub>2</sub> O nanoparticles	4	0.8	90	98.93	277.85	[34]
pectin	4	1.0	24H	-	120	[35]
Adsorbent	pH	Adsorbent mass (g/L)	Equilibrium time (min)	Removal percent%	q <sub>max</sub> (mg/g) for cefixime	Ref
Co-Fe LDH/Cellulose	5	0.06	15	91.16	208	This work
chitosan@polyacrylamide@ZIF-8	4	0.015	30	90	588	[31]
chitosan 10B	5	0.03	240	-	37.04 μmol/g	[30]
HKUST-1/ZIF-8	7		240	-	110	[25]

Green chemistry is a scientific approach that focuses on designing chemical products and processes that minimize the use of hazardous substances and reduce the environmental impact. It promotes sustainability, reduces waste, and conserves energy and resources. Some of the principles of green chemistry include the use of renewable raw materials, the development of safer and more efficient chemical reactions, and the creation of products that are biodegradable and non-toxic. The adoption of green chemistry practices can lead to significant improvements in environmental and human health outcomes, as well as economic benefits [41,42].

## Materials and Methods

Cefixime (CFX, C<sub>16</sub>H<sub>15</sub>N<sub>5</sub>O<sub>7</sub>S<sub>2</sub>; Assay 95–110 %) was purchased from Arshine Pharmaceutical Co., Limited, China. Sulfamethoxazole (SMX, C<sub>10</sub>H<sub>11</sub>N<sub>3</sub>O<sub>3</sub>S; Assay 99.11%) was purchased from Anant Pharmaceuticals Pvt. Ltd., India. Cobalt chloride hexahydrate (CoCl<sub>2</sub>·6H<sub>2</sub>O), iron chloride (FeCl<sub>3</sub>), and phosphoric acid were purchased from Sigma-Aldrich. Hydroxyethyl cellulose (HEC) (Product number 434965) with an average molecular weight of 90,000 was also purchased from Sigma-Aldrich. All preparations were made using twice distilled water. Sodium

hydroxide and ethanol with a purity of 99.8% from Sigma-Aldrich, and hydrochloric acid (ACS BASIC Scharlau) were used. All other chemicals used are summarized in Table 2.

**Table 2:** List of Chemicals used in the experimental section of this work.

Chemical	Company	Chemical structure	Purity %	CAS number
Sodium hydroxide	Merck	NaOH		1310-73-2
HCl	Piochem	HCL	37%	7647-01-0
Hydroxy ethyl cellulose HEC	Sigma-Aldrich	C <sub>29</sub> H <sub>52</sub> O <sub>21</sub>	83-95%	9004-62-0
Cobalt nitrate	Piochem	Co(NO <sub>3</sub> ) <sub>2</sub> .H <sub>2</sub> O	97-101%	10026-22-9
Ferric nitrate	Alpha chemica	Fe(NO <sub>3</sub> ) <sub>3</sub> .9H <sub>2</sub> O	98%	10421-48-4
Ethanol	Sigma -Aldrich	CH <sub>3</sub> CH <sub>2</sub> OH	99.8%	64-17-5
Cefixime	Hikma Pharmaceutical Company, Beni-Suef, Egypt	C <sub>16</sub> H <sub>15</sub> N <sub>5</sub> O <sub>7</sub> S <sub>2</sub>	95–110%	79350-37-1
Sulfamethoxazole	Anant Pharmaceuticals Pvt. Ltd., India.	C <sub>10</sub> H <sub>11</sub> N <sub>3</sub> O <sub>3</sub> S	99.11%	723-46-6

### Preparation of Cellulose-based Co-Fe LDH adsorbent

2 g of HEC were swollen in a solution containing 0.189 mol of urea and 1 M sodium hydroxide. The swollen HEC was then added dropwise to a 250 ml beaker containing 100 ml of an aqueous solution with 0.3 M Co<sup>2+</sup> and 0.1 M Fe<sup>3+</sup> at a rate of 1 ml/min, using the co-precipitation method with constant stirring. A 0.5 M NaOH solution was then added through a titration system under continuous stirring until the pH reached 10.0. The resulting precipitate was aged for 24 hours at 70 °C. The suspension was then centrifuged to separate the precipitate, washed several times with distilled water, and finally with ethanol until the pH reached 7. The formed precipitate was then dried at 50°C in an oven for 24 hours.

### Materials Characterization

The prepared material was characterized using various tools. Analytical (Empyrean) X-ray diffractometer with Cu-K $\alpha$  radiation was used to determine the crystallinity and structural composition of the synthesized cellulose-based LDH. The diffractometer operated at a current of 35 mA and voltage of 40 kV, scanning at a rate of 8° min<sup>-1</sup> from 5° to 80° (2 $\theta$ ). Additionally, the infrared spectra of the prepared material were recorded using a Bruker-Vertex 70 spectrometer in the wave number range of 4000-400 cm<sup>-1</sup> after homogenizing 0.50 mg of each material with 300 mg of optically high purity KBr and pressing the mixture under 10 ton/cm<sup>2</sup> for 15 min. The microstructure and morphology of the synthesized LDH/ Cellulose were investigated using a Field Emission Scanning Electron Microscope (FESEM). The elemental composition of the nanocomposite was assessed using Energy Dispersive Spectroscopy (EDX); the BET specific pore volume and specific surface area of the Co-Fe LDH/Cellulose were all determined by N<sub>2</sub> adsorption and an automated surface analyzer (TriStar II 3020, Micrometrics, USA). The hydrodynamic particle size and zeta potential.

## Adsorption Study

A series of diluted concentrations (5–500 µg/ml) were prepared from a stock standard solution of 1000 µg/ml to create a calibration curve at room temperature for each drug. To examine the effect of pH on the adsorption process, six 50 ml falcon tubes were prepared with 0.05 g of the synthetic adsorbent (Co-Fe LDH/Cellulose) and 50 ppm of each of SMX and CFX. The pH of the solutions was adjusted to pHs of 3, 5, 7, and 9 using 0.1 N NaOH or 0.1 N HCl. The tubes were then placed on an orbital shaker for 24 hours at 250 rpm. The effect of the dose of adsorbent on the adsorption process was examined at a constant concentration of 50 ppm for each of SMX and CFX using different doses ranging from 0.02g to 0.10 g. The effect of drug concentration was also examined using different concentrations ranging from 0 ppm to 100 ppm. The residual concentrations of antibiotic residues were measured using a double beam UV–visible spectrophotometer (UV-2600 UV-Vis Spectrophotometer, Shimadzu) at wavelength 265 nm, 288 nm for Sulfamethoxazole (SMX); Cefixime (CFX) respectively. The amount of adsorbed drugs per gram and the removal percentage of Co-Fe LDH/Cellulose ( $Q_e$ ) were determined using the equations.

$$Q_e = \frac{(C_o - C_t)V}{w} \quad (1)$$

$$\text{Removal percent} = \frac{C_o - C_t}{C_o} \times 100 \quad (2)$$

Adsorption isotherm models and different kinetic models were investigated to study the adsorption of the concerned drugs onto the Co-Fe LDH/Cellulose. For adsorption isotherm experiments, eight isotherm models were investigated to fit the experimental results for both SMX and CFX. Finally, SMX and CFX ions adsorption kinetics were investigated and then fitted to various kinetic models.

Regeneration experiments: As desorbents, ethanol, methanol, isopropanol, and acetonitrile were used in regeneration experiments. Ten milligrams of waste adsorbent were added to twenty milliliters of desorbent reagent. These samples were then shaken for 24 hours at 25 °C at 120 rpm. The regeneration efficiency was then calculated by measuring the quantities of SMX using ultraviolet-visible spectrophotometry. Reuse experiments were conducted where the adsorbent was regenerated for five cycles and the removal efficiency was calculated for each cycle.

Real sample investigation: Real sample treatment the experiments were performing by three different real water samples (tap water, River-Nile water and ground water) was collected. We spiked the collected samples by 5 ppm of SMX then the pH and performing the removal process using optimum dose of applied Co-Fe LDH/Cellulose for 3 hrs.

## The Assessment of Environmental Sustainability

### Analytical Eco-Scale Assessments (ESA)

Conducting sustainability assessments requires analytical eco-scale tools. A global penalty score is used to assess sustainability, which accounts for many aspects, such as waste generation, energy consumption, and reagent

consumption [43]. A perfect score of 100 is assumed, but the actual number is lower [44]. If the system scores fewer than 50 points, it is classified as "sufficient green," if it scores between 50 and 75 points, and if it scores more than 75 points, it is classified as "superior green." Environmental sustainability can be measured by a greenness profile [45].

### **AGREE tool**

Ecological sustainability and comprehensive criteria are considered in the AGREE evaluation process. There are 12 GAC essential principles, scored numerically from 0 to 1. For each concept of ecological sustainability, a score of 1 is assigned. Each benchmark's performance level is represented in the graphic by a red, yellow, and green gradation. A direct correlation exists between section diameters and each parameter value [46].

### **AGREEprep tool**

A sample's strength is determined by its preparation, which is crucial in the analytical process. With AGREEPrep, sample preparation has a minimal ecological footprint. Analyzing the environment and handling samples are integrated with environmentally conscious practices. GAC's 12-point guidance was deviated from by AGREEprep. GSP includes the 10 principles as part of AGREEPrep. By preparing samples environmentally consciously, Wojnowski et al. (2022) adhere to a sustainable approach. Sample preparation techniques are quantified using AGREEPrep. To optimize sample preparation, AGREEprep combines environmental responsibility and evaluation. There are ten steps involved in evaluating someone's competency. Scores of 0 and 1 represent the minimum and maximum, respectively. Throughout the ten areas, there are graphic icons. AGREEPrep's success depends on several key factors. A laboratory must consider the presence of dangerous substances, the amount of waste generated, the rate at which samples will be used per hour, and the energy consumption level before sending samples to the lab. Prepare for the test by considering all these factors [47].

### **In vitro cytotoxicity study**

#### **MTT Assay**

The MTS assay was performed to determine the cytotoxicity level of Co-Fe LDH/Cellulose, Co-Fe LDH/Cellulose-SMX, and Co-Fe LDH/Cellulose-CFX on Vero cells as previously described [48]. MTT assay evaluates cell viability by measuring the activity of enzymes that convert the MTT reagent to formazan, which produces a purple color. Cells ( $2 \times 10^3$ ) were seeded into each well of a multi-well plate in 200  $\mu$ L of growth medium and incubated for 24 h at 37°C with 5% CO<sub>2</sub>. This allows the cells to adhere and acclimatize. The samples being tested for cytotoxicity were then introduced. After an appropriate incubation period, the MTT reagent was added to each well and further incubated. After the initial 24-hour incubation period, the original culture medium containing any non-adherent cells was removed from each well and replaced with fresh medium to maintain the total volume at 200  $\mu$ L per well. The test samples were cut into small 4 x 4 mm squares, sterilized by soaking in 70% ethanol followed by UV light exposure for 8 hours, and then placed into the wells with the adhered cells. This was done separately for

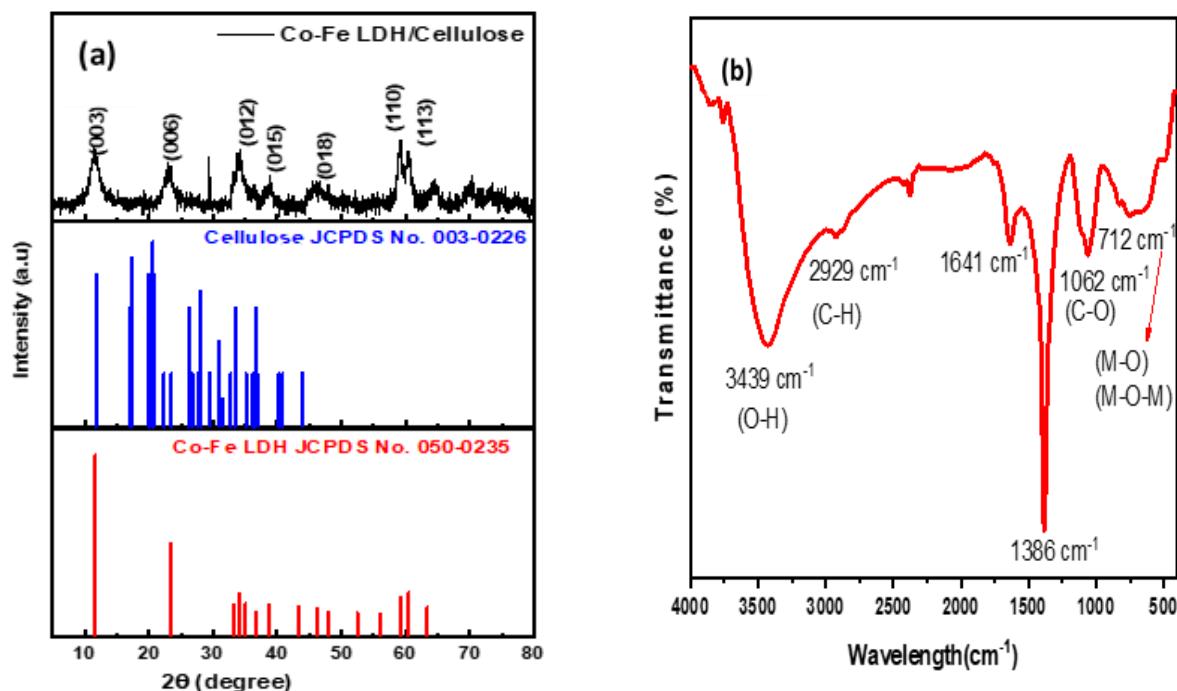
incubation periods of 24h. At the end of each incubation period, the medium was removed and MTT solution at 0.5 mg/mL in serum-free medium was added to each well. The plates were incubated for 4 hours in the dark at 37°C allowing viable cells to metabolize MTT into purple formazan crystals. The MTT solution was then carefully aspirated and DMSO was added to dissolve the formazan crystals. Absorbance was measured at 570 nm using a microplate reader to quantify the soluble formazan production, which is proportional to the number of viable cells. Cell viability was calculated using the formula:

$$\% \text{ viability} = (\text{Absorbance of sample well} / \text{Absorbance of control well}) \times 100$$

## Results and Discussion

### Adsorbent Characterization

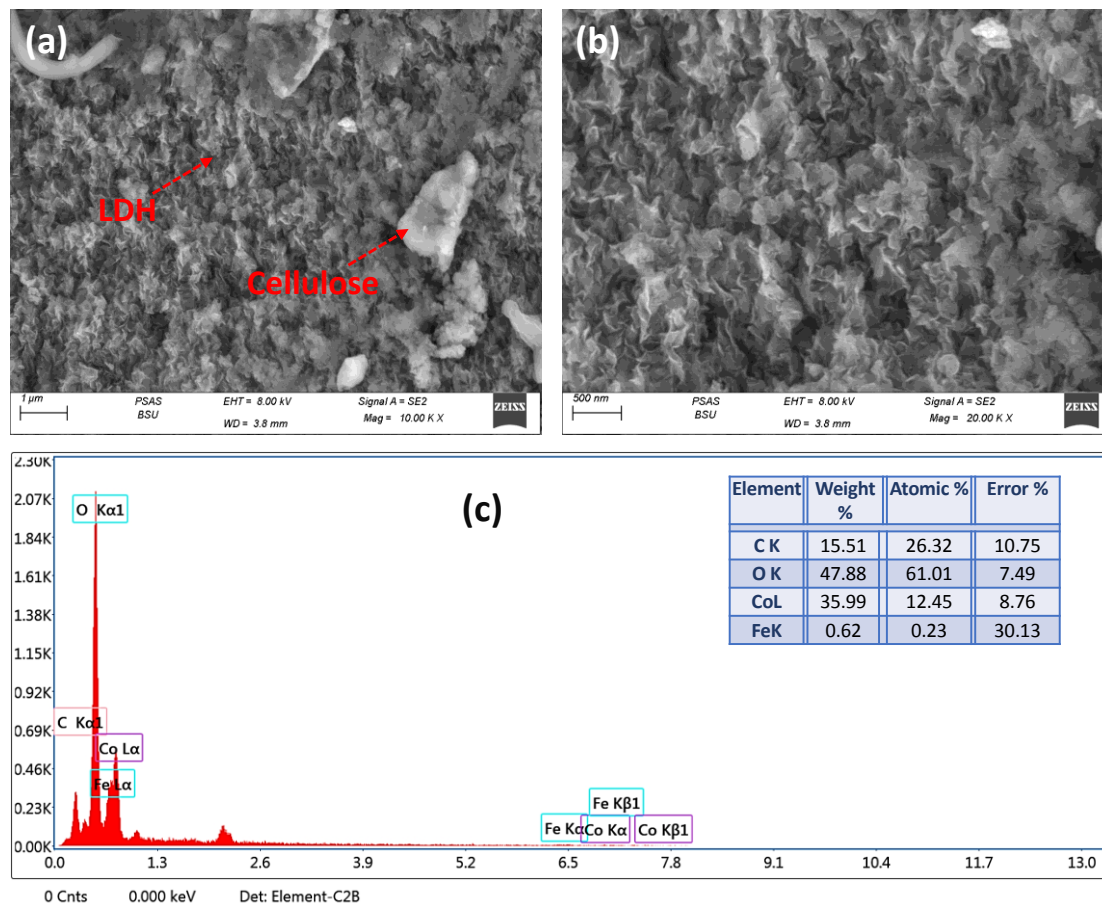
**Figure 1:** (a, b) XRD and FTIR spectra of Co-Fe LDH/Cellulose nanocomposite.



The x-ray diffraction of the Co-Fe LDH/Cellulose is shown in Figure 1. The XRD patterns show that the LDH material has typical peaks at  $2\theta = 11.4^\circ, 23.3^\circ, 33.1^\circ, 34.1^\circ, 39^\circ, 45.9^\circ, 59.1^\circ,$  and  $60.3^\circ$ , respectively, in agreement with the (003), (006), (101), (012), (015), (018), (110), and (113) planes (JCPDS Card No. 00-050-0235) [48]. The peaks at  $2\theta = 27.8^\circ$  and  $29.4^\circ$ , which matched the (013) and (-222) planes, respectively, according to JCPDS card No. 003-0226 verified the presence of cellulose [49]. The crystallite size of the prepared Co-Fe LDH/Cellulose was identified by applying the Scherrer equation,  $CZ = (0.94 \lambda) / (\beta \cos \theta)$ ,  $\lambda$  is the wavelength of incident X-ray ( $\text{CuK}\alpha = 0.154 \text{ nm}$ ),  $\beta$  is the full width at half maximum and  $\theta$  is the Bragg's angle. The Co-Fe LDH/Cellulose 'CZ was 4.79 nm.

The FTIR test is often used to determine the functional groups present in a nanocomposite [50]. Figure 1(b) displays the FTIR spectra for Co-Fe LDH/Cellulose shows that Co-Fe LDH/Cellulose provides a broad band at  $3431\text{ cm}^{-1}$ , and a band at  $1630\text{ cm}^{-1}$  which are attributed to O-H groups [51,52]. The C-H stretching vibrations in cellulose is observed at  $2920\text{ cm}^{-1}$  [53]. The band at  $1383\text{ cm}^{-1}$  is ascribed to the stretching vibration of the  $(\text{NO}_3^-)$  group in LDH [54]. The C-O-C groups show a distinctive band at  $1052\text{ cm}^{-1}$  due to the glycosidic units in cellulose [55]. The additional bands at  $714$  and  $482\text{ cm}^{-1}$  indicate M-O, M-OH, and O-M-O vibrations ( $\text{M}=\text{Co}^{2+}$  and  $\text{Fe}^{3+}$ ) [56].

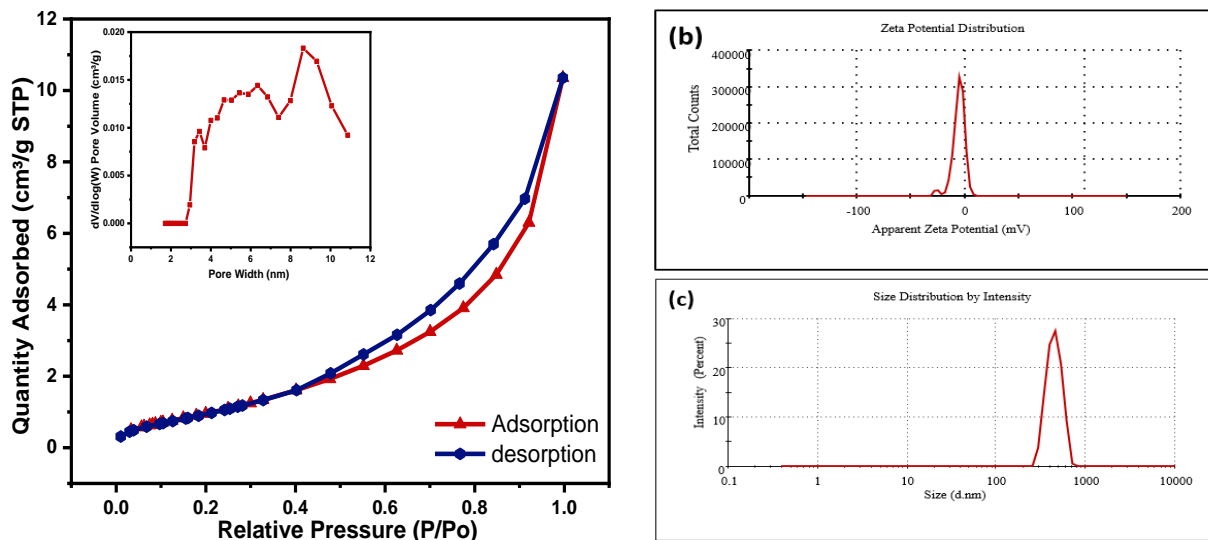
**Figure 2:** (a, b) SEM images at different magnifications and(c) EDX spectrum of synthesized Co-Fe LDH/Cellulose.



SEM images of the morphological structures of Co-Fe LDH/Cellulose was analyzed at different magnifications as displayed in Fig .2 (a-b). Cellulose material was applied on Co-Fe LDH to create irregular sized and distributed particles ranged between 500:1300 nm. The Co-Fe LDH is appeared as composed of layers, as is characteristic of the LDH materials [57]. Supporting for the intercalation mechanism between the Co-Fe LDH/Cellulose with SMX and CFX is suggested by the channels and pits features of the LDH and the porous structures of cellulose material.

LDH/Cellulose's surface element types and contents were identified using EDX patterns as shown in Fig. 2c. C and O peaks on Co-Fe LDH/Cellulose showed that the cellulose had been successfully introduced onto the Co-Fe LDH.

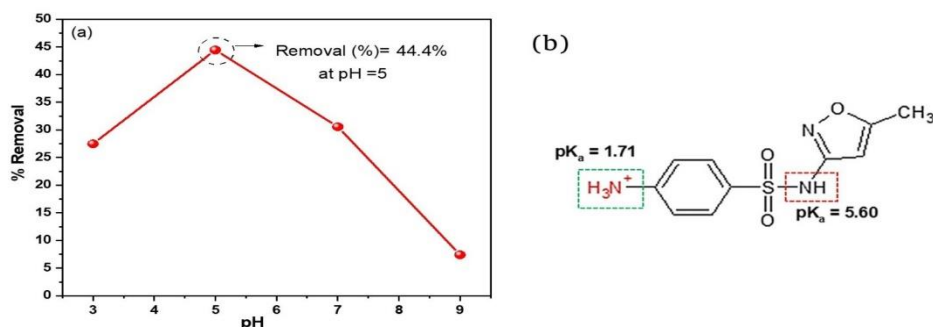
**Figure 3:** (a) N<sub>2</sub> adsorption/desorption isotherms (inset is BJH pore size distributions), (b) zeta potential and (c) zeta size of Co-Fe LDH/Cellulose.

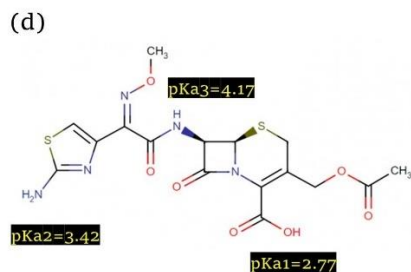
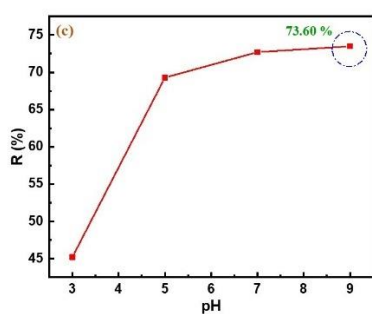


The Co-Fe LDH/Cellulose material's Brunauer-Emmet-Teller (BET) surface area was determined using N<sub>2</sub> adsorption-desorption isotherms as displayed in Fig. 3a. As to the IUPAC classification, Co-Fe LDH/Cellulose exhibits an isotherm of type (IV) including an H3 hysteresis loop [58]. For Co-Fe LDH/Cellulose, the result is particle aggregation in sheets with holes, including slits of various forms. In materials with micropores, an H3 hysteresis loop is often seen. and the Barrett-Joyner-Hanlenda (BJH) theory showed the pore size distribution. Co-Fe LDH/Cellulose's adsorption isotherm measurements gave us the high specific surface area  $S_{BET}$  of 15.46 m<sup>2</sup> g<sup>-1</sup>. The BJH pore size and BJH pore volume 0.015468 cm<sup>3</sup> g<sup>-1</sup>. The presence of a hysteric loop indicates the material's mesoporous structure, which is between 2 and 50 nm. This is confirmed by the BJH pore size of 15.08368 nm, which shows the Co-Fe LDH/Cellulose's effective adsorption capacity [27,59].

Zeta potential studies demonstrate the stability of the synthesized material. It is a measurement of the mutual attraction or repulsion of electrically charged particles in a solution, Fig. 3b. The Co/Fe/LDH-Cellulose zeta potential measurement, which was -5.71 mV, indicates that the produced nanoparticles have a high degree of stability. The Co-Fe LDH/Cellulose's size distribution intensity was reported in Fig. 3c to be 622 nm.

### Adsorption Study.

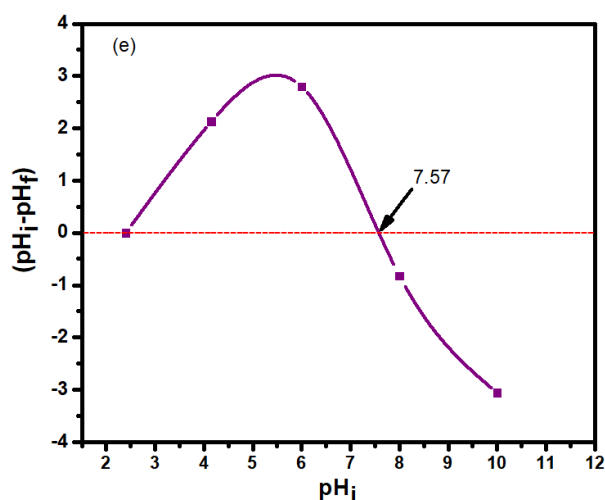




We tested the adsorption process of the SMX and CFX by using Co-Fe LDH/Cellulose nanocomposite at optimized parameters as pH, Co-Fe LDH/Cellulose dose, concentration, and contact time. Adsorbent and adsorbate surfaces both have functions that are pH-dependent. Therefore, it is important to optimize the pH of the adsorption media. For this, 10 mg of Co-Fe LDH/Cellulose were added to 20 mg/L SMX or CFX solutions and the pH was adjusted at 3, 5, 7, and 9 for 24 hours. Maximum percentage removal (44.4%) was discovered to occur at the pH range of 5. SMX is therefore selected for adsorption at pH 5. Maximum percentage removal (73.60%) for CFX was discovered to occur at the pH range of 9. CFX is therefore selected for adsorption at pH 9.

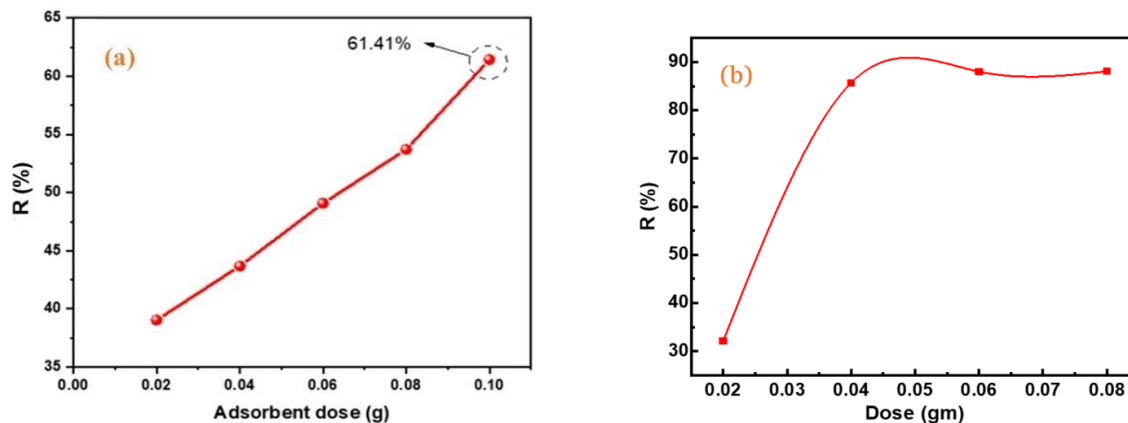
The effect of pH on SMX and CFX adsorption is shown in Fig. 4 (a& c). SMX have two dissociation constants at  $pK_1 = 1.71$ ,  $pK_2 = 5.60$  [60]. At low pH values, SMX is negatively charged (Fig. 4b) and the adsorbent was positive (Fig. 4e). The electrostatic attraction between both SMX and Co-Fe LDH/Cellulose is the main reason for the high RE% at pH=5. In the pH beyond 5, the charge of Co-Fe LDH/Cellulose is changed to negative (as shown in Fig. 4e) and SMX becomes negatively charged completely. Therefore, the electrostatic attraction plays a significant role in increasing the observable RE% at pH 5.

**Figure 4:** The effect of the pH on the removal efficiency of SMX (a) and CFX (c); chemical structure including the dissociation constants of SMX (b) and CFX (d) and the charge of the adsorbent in different pH (e).



CFX has three dissociation constants at  $pK_1 = 2.77$ ,  $pK_2 = 3.42$ , and  $pK_3 = 4.17$  [61,] therefore increasing pH above  $pK_a$  leads to negative charge formation on CFX (Fig.4d). The removal percent reach 73.60% at pH 9, The electrostatic attraction between both CFX and the adsorbent is not the main reason for the low RE% at pH=3. the other intermolecular forces may be plays a significant role in increasing the observable RE% at pH 9 like hydrogen bonding [62].

**Figure 5:** The effect of the Co-Fe LDH/Cellulose (g) on the removal efficiency of SMX (a) and CFX (c).

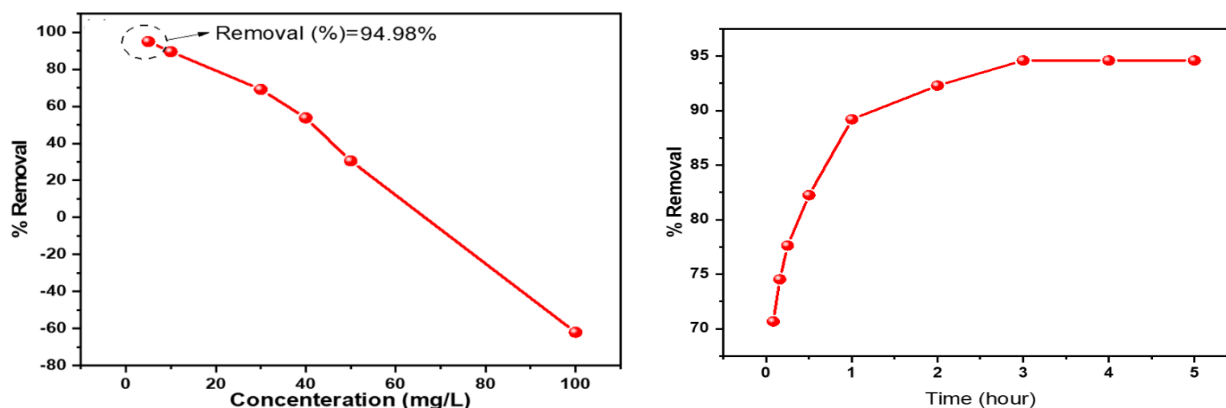


To evaluate the impact of the adsorbent dosage, Co-Fe LDH/Cellulose concentrations ranging at 20, 40, 60, 80, and 100 mg were equilibrated for 24 hours with 20 mg/L SMX at pH 5 and CFX at pH 9. The percentage of SMX removal was shown to rise with increasing amounts of adsorbent (Fig. 5(a-b)). For subsequent adsorption trials, the adsorption dose of 100 mg was established with percentage removal of 61.41%. For the CFX the percentage of its removal was shown to rise with increasing amounts of adsorbent (Fig. 5(a-b)). For subsequent adsorption trials, the adsorption dose of 50 mg was established with percentage removal of 91.16 %.

Effect of Concentration of SMX and CFX were studied using optimized 100 mg for SMX and 50 mg for CFX of Co-Fe LDH/Cellulose was equilibrated with concentration of drug ranging from 5 to 1000 mg/L at pH 5. For the adsorption investigations, a starting concentration of 5 mg/L SMX and CFX solution was chosen. Because there are fewer drug species than adsorption sites, it is assumed that the adsorption efficiency increases at lower drug concentrations. As the concentration of the pollutant solution increases, on the other hand, more pollutant molecules are present, the adsorption sites become fixed, and the rate of adsorption increases less (Fig. 6a).

To investigate the effect of contact time on the percentage removal of SMX and CFX, contact times ranging from 0.00 to 5 hours were used. To do this, 200 mL of drug concentration of 50 mg/L equilibrated with 100 mg of Co-Fe LDH/Cellulose. It was noted that the percentage removal of drug rapidly increased with the passage of time. The Co-Fe LDH/Cellulose surface had more accessible adsorption sites at the start of the experiment, and after 3 hours it reached equilibrium for SMX (Fig. 6b).

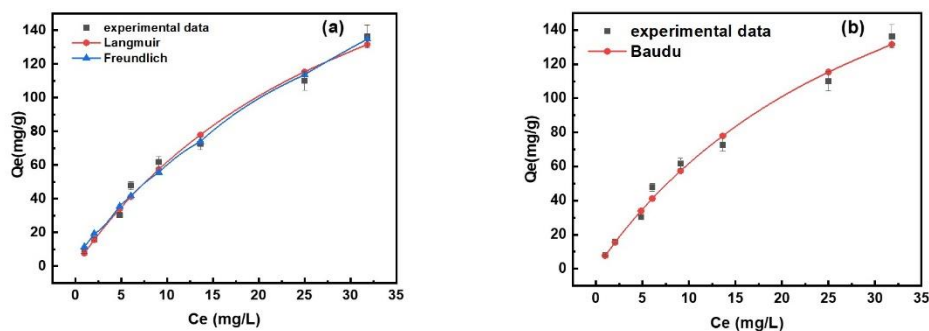
**Figure 6:** (a) effect of concentration of the SMX on the removal percent using 100 mg of Co-Fe LDH/Cellulose and (b) effect of time on the removal percent of SMX using 100 mg of Co-Fe LDH/Cellulose.



### Adsorption Isotherm Investigations

Adsorption isotherms may be used to understand how molecules of pollutant interact with the as-prepared adsorbent surface at equilibrium. In order to show how sulfamethoxazole and cefixime adsorb on Co-Fe LDH/Cellulose surfaces, the non-linear fitting method was employed equilibrium data for Langmuir, Freundlich, Dubinin–Radushkevich, Baudu, Langmuir-Freundlich and Redlich Peterson isotherm models. Equation (Table 3) provides a summary of the adsorption isotherm constant correlation coefficient values, and Fig. 7 displays their plots. Concerning the sorption of sulfamethoxazole, the obtained  $R^2$  0.988 values of Langmuir models and cefixime, the obtained  $R^2 = 0.998$  values of Langmuir models, respectively, from Table 3. Since the  $R^2 = 0.994$  values for the Freundlich isotherm were higher compared to those with the other isotherm model for sulfamethoxazole adsorption, where in case of cefixime  $R^2 = 0.998$  for Langmuir isotherm model. It can be concluded that the Langmuir isotherm well fitted in case of cefixime and Freundlich sufficiently represent the sorption characteristics of sulfamethoxazole on Co-Fe LDH/Cellulose surfaces. According to the calculations using Langmuir isotherm revealed that the highest sulfamethoxazole surfaces adsorption ability of was 272.13, and 208.00 mg/g for cefixime, respectively.

**Figure 7:** Non linearized fitting of different isotherm models for the adsorption of (a-c) sulfamethoxazole - (d) cefixime (d-f) onto Co-Fe LDH/Cellulose composite.



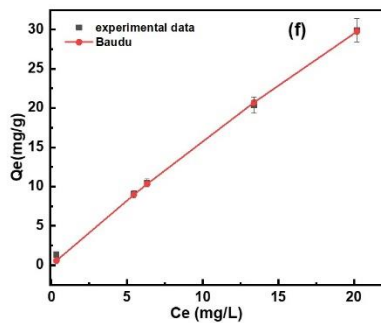
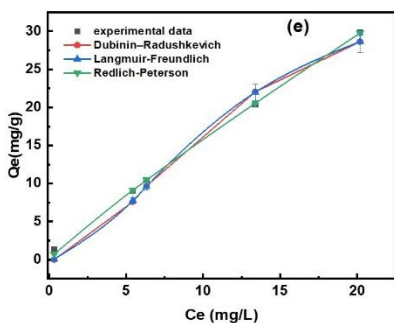
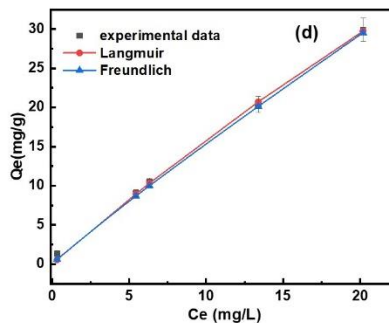
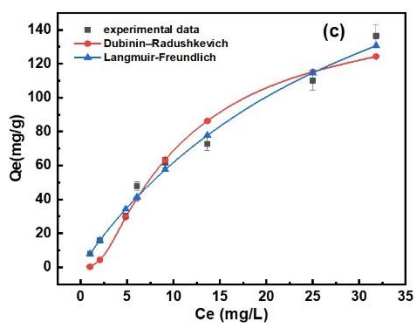


**Table 3:** A summary of the adsorption isotherm constant correlation coefficient values and the model equations.

Model	Parameter	sulfamethoxazole	cefixime
Langmuir $q_e = q_{max} \frac{K_L C_e}{1 + K_L C_e}$	$q_{max}$	272.1337	208.0024
	$K_L$	0.0294	0.0082
	$R^2$	0.9889	0.9983
Freundlich $q_e = K_f C_e^{1/n}$	$1/n$	0.7079	0.9338
	$K_f$	11.6427	1.7847
	$R^2$	0.9948	0.9579
	AT	0.3551	1.007
	$R^2$	0.8718	0.8472

Dubinin–Radushkevich $q_e = q_{max} \exp(-K_{DR} \varepsilon^2)$	$q_{max}$	165.0706	48.7814
	$K_{ad}$	0.0018	0.0022
	$R^2$	0.9574	0.9679
Langmuir-Freundlich $q_e = \frac{q_{max}(K_{LF}C_e)^{MLF}}{1+(K_{LF}C_e)^{MLF}}$	$q_{MLF}$	273.8824	39.3589
	$K_{LF}$	0.0286	0.0850
	$M_{LF}$	0.9850	1.8205
	$R^2$	0.9891	0.9660
Redlich-Peterson $q_e = \frac{K_R C_e}{1+a_R C_e^{\beta R}}$	$K_R$	395.8314	253.3730
	$a_R$	33.3760	126.8887
	$\beta$	0.2893	0.0989
	$R^2$	0.7370	0.9991
Baudu $q_e = \frac{q_{max} b_0 C_e^{1+x+y}}{1+b_0 C_e^{1+x}}$	$q_m$	272.0736989	207.9381
	$b_0$	0.029455705	0.0082
	$x$	0	0
	$y$	0	0
	$R^2$	0.9889	0.9983

### Adsorption Kinetics Investigations

In Fig. 8, the equilibrium adsorption of SLF and CFX adsorption using Co-Fe LDH/Cellulose composite shown as a function of time. The equilibrium adsorption of SLF or CFX using prepared adsorbent has elevated with the growth of time from 0 to 10 minutes. The rate of adsorption in the early times had a high speed, and after 50 min did not change significantly. This state may be a direct result of the adsorption power of the drug residues in the aqueous media, which has a fast diffusion on the outer surface of the desired adsorbents<sup>63</sup>. The increase in the sorption efficiency in the initial times can be due to the significant presence of sites in the adsorber feature<sup>64</sup>. To analyze the adsorption behavior of SLF or CFX from the water media using Co-Fe LDH/Callose, pseudo-first-order (PFO), pseudo-second-order (PSO), intra-particle diffusion (IPD) models, avrami (AV) and mixed 1,2 order (MO) were

investigated, whose non-linear relationship is presented in Table 4. The kinetics rate constants of all models PFO, PSO, AV, MO and IPD, respectively,  $q_e,cal$  (mg/g) denotes the equilibrium sorption capacity,  $q_e$  and  $q_t$  (mg/g) are the sorption capacity at the moment of equilibrium and each moment, respectively. The non-linear relationship of the kinetics models of all model for the SLF and CFX adsorption using Co-Fe LDH/Cellulose, and the corresponding constants and variables are listed in Table 4. The value of  $R^2$  and  $q_e,cal$  for MO is lower compared to other kinetic models. It should be noted that the  $R^2$  parameter value determined using the models is more than 0.9 except IPD, which illustrates that SLF or CFX adsorption using the desired LDH composite is a complex reaction in which physical and chemical adsorption is performed simultaneously. These two processes have synergistic impacts during the adsorption [65].

**Figure 8:** Kinetic study plots with different non liner kinetic models for sulfamethoxazole (a) and cefixime (b) adsorption onto Co-Fe LDH/Cellulose composite.

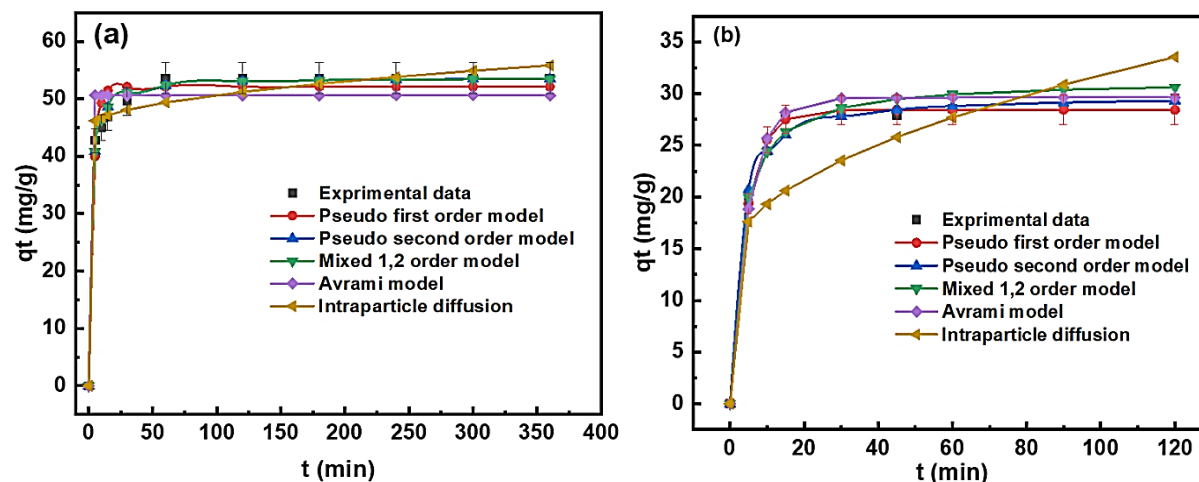


**Table 4:** A summary of nonlinear kinetic models for sulfamethoxazole (a) and cefixime (b) adsorption onto Co-Fe LDH/Cellulose composite.

Kinetic models	Equation	Parameter s	sulfamethoxazole	cefixime
Pseudo first Order	$q_t = q_e (1 - e^{-k_1 t})$	$K_1$	0.2910	0.2284
		$Q_e$	52.1230	28.4382
		$R^2$	0.8191	0.9949
Pseudo second Order	$q_t = \frac{q_e^2 k_2 t}{1 + q_e k_2 t}$	$K_2$	0.0117	1.52E-02
		$Q_e$	53.7259	29.8537

		R <sup>2</sup>	0.9646	0.9941
Mixed 1,2 order	$q_t = q_e \frac{(1-\exp(-kt))}{1-f_2\exp(-kt)}$	K	0.0024	0.0015
		Q <sub>e</sub>	53.6324	31.2774
		F <sub>2</sub>	0.9961	0.9954
		R <sup>2</sup>	0.9645	0.9560
Avrami	$q_t = q_e[1-\exp(-k_{av}t)^{n_{av}}]$	Q <sub>e</sub>	50.5909	29.6198
		K <sub>av</sub>	3	0.4625
		n <sub>av</sub>	5.4720	0.4371
		R <sup>2</sup>	0.9341	0.9393
Intraparticle diffusion	$q_t = K_{ip}\sqrt{t} + C_{ip}$	K <sub>ip</sub>	0.5765	1.8271
		C <sub>ip</sub>	44.9035	13.5395
		R <sup>2</sup>	0.8700	0.6250

### Recyclability of the Nano-Adsorbent

It is one of the most important factors in examining the reusability of the adsorbents used in order to assess their economic situation. The reuse of the adsorbent in SMX removal as representative example, as shown in Fig. 9, where almost no detectable loss of removal efficiency was observed in three consecutive cycles, indicating a favorable reusability of this adsorbent. After three cycles, the efficiency of Co-Fe LDH/Cellulose for SMX decreased to 50 %.

### Cost Estimation of the Prepared Adsorbent

**Table 5:** Cost estimation details of the prepared adsorbent.

Material	Purchased quantity (g)	Total purchase cost (USD)	purchasing cost (USD/g)	Used quantity (g or mL)	cost of used quantity (USD)
HEC	25	3.8	0.152	2	0.3
Urea	500	10.95	0.0219	11.34	0.23
NaOH	100	22	0.22	3.5	0.77
Cobalt salt	100	12.6	0.126	5.5	0.693

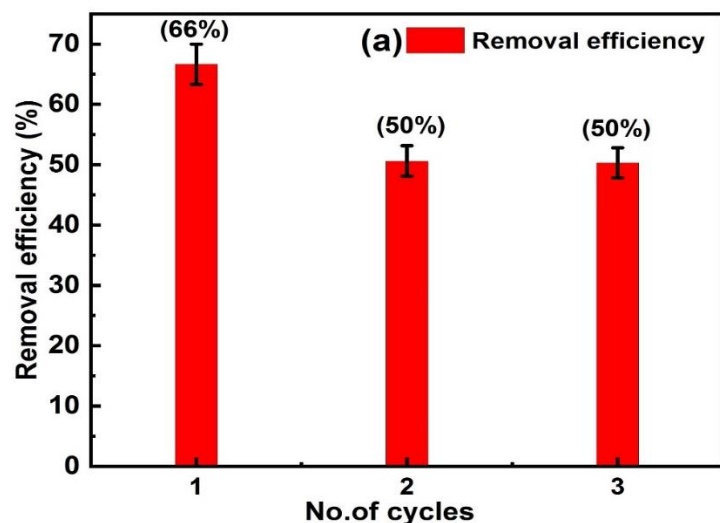
Ferric salt	100	22	0.22	2.42	0.5
Equipment	Time (h)	Max. power (kW)	unit cost of power	Energy cost (USD)	
Stirrer	24	1	0.16	3.84	
dryer	24	1	0.16	3.84	
centrifuge	1	1	0.16	0.08	
total				10.3	USD
yield				3	g
cost				3.44	USD/g

Cost estimation of prepared adsorbents is one of important tools of analysis of performance. That is because, cheap adsorbents offer an advantage towards real-life applications. For this adsorbent, HEC, urea, NaOH, Cobalt and ferric salts were used during synthesis procedure. These chemicals costed a sum of 2.55 USD, where the details of cost of each chemical are shown in table 5. As for energy requirements, a stirrer (equipped with hot plate), dryer and centrifuge were used and their total energy consumption accounted for 7.76 USD. The yield of this adsorbent was 3 g and hence its specific cost (cost per unit mass) was calculated to be approximately 3.44 USD/g. To further decrease the cost of this adsorbent, renewable energy sources may be considered for drying and/or providing energy for stirring since energy costs represents almost three folds that of materials costs, which account for 75% of the overall cost.

### Real Water Samples Analysis

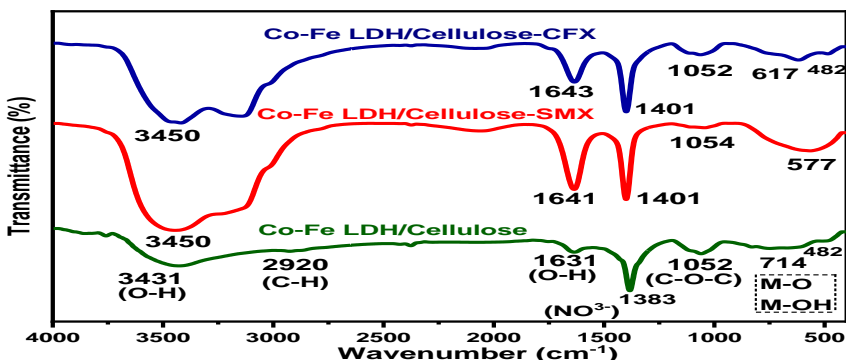
The existing removal of SMX using collected real water sources (tap water, river Nile water and groundwater samples) by spiking 5 ppm, pH 5 and 0.10 g Co-Fe LDH/Cellulose nanocomposite was 59% for waste water, 50% for river and 50% for tap water.

**Figure 9:** the reuse study of Co-Fe LDH/Cellulose for SMX removal using 100 mg of adsorbent and 5 ppm of SMX.



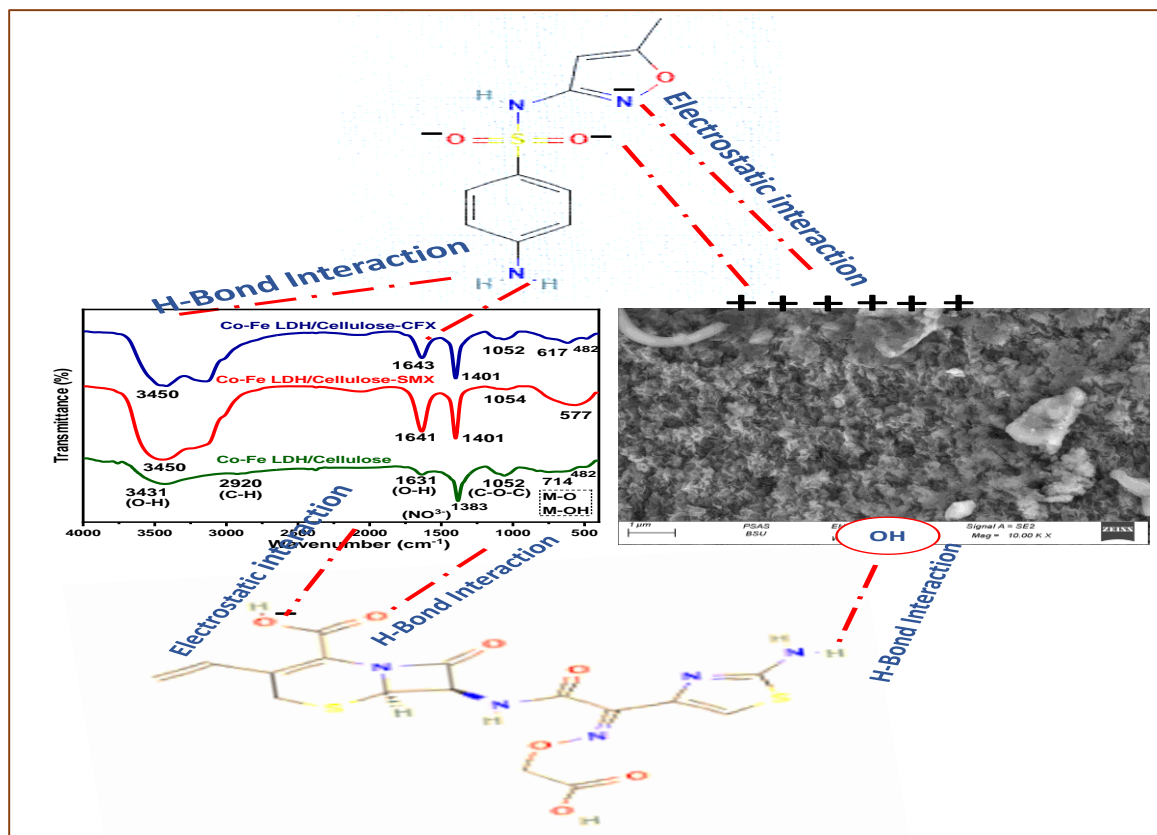
### Possible Adsorption Mechanisms

**Figure 10:** FTIR spectra of Co-Fe LDH/Cellulose, Co-Fe LDH/Cellulose-SMX, and Co-Fe LDH/Cellulose-CFX.



One of often described adsorption processes in the literature involving the oxygen-functional groups of adsorbents and specific target groups of adsorbates is the hydrogen bond interaction. We can confirm this interaction by comparing the FTIR of the adsorbent before and after the medicines are adsorbed (fig. 10). With a more broadened and intensely shaped pattern, the OH groups' wavenumber shifted from 3431  $\text{cm}^{-1}$  (Co-Fe LDH/Cellulose) to 3450  $\text{cm}^{-1}$  (LDH/Cellulose-SMX and Co-Fe LDH/Cellulose-CFX). Additionally, the same group at a wavenumber of 1631  $\text{cm}^{-1}$  (Co-Fe LDH/Cellulose) shifted to 1641  $\text{cm}^{-1}$  (LDH/Cellulose-SMX) and to 1643  $\text{cm}^{-1}$  (Co-Fe LDH/Cellulose-CFX). This indicates that those groups on the surface of Co-Fe LDH/Cellulose were essential in the adsorption of SMX and CFX through hydrogen bonding interactions.

**Figure 11:** Adsorption mechanism of Co-Fe LDH/Cellulose with SMX and CFX.



Electrostatic or acid-base interactions are common ways in which pharmacological contaminants are adsorbed. The contaminant and adsorbent structures had diametrically opposed functional groups: the former had an acidic group while the latter had a basic group. This resulted in the development of this mechanism. The anionic group was connected to the negatively charged SMX and CFX through the positively charged LDH via these electrostatic interactions. The FTIR spectra, in particular the wave number of the nitrate group at  $1383\text{ cm}^{-1}$ , which moved to  $1401\text{ cm}^{-1}$  following SMX and CFX adsorption, may be used to prove this. The mechanism was explained in Fig. 11. In addition, the CFX has N atoms and SMX has N and S atoms, which can form hydrogen bonds (chemical bonds) with H atoms in the structure of Co-Fe LDH/Cellulose and form dipole-dipole bonds with oxygen atoms. the creation of  $\pi$ - $\pi$  stacking is another additional factor that can improve the removal efficiency. It should be mentioned that LDH compounds can remove drug residues molecules through electrostatic, hydrogen bonds, and  $\pi$ - $\pi$  interactions.

## Quantification of Environmental Sustainability: An Assessment of Techniques

### Analytical Eco-Scale Assessments (ESA)

The ESA tool determined a precision penalty point of 75, indicating the technique is both ecologically sustainable and environmentally friendly. As well as presenting a visual representation of the penalties, Table 6 provides a concise and comprehensive overview of the evaluation results.

**Table 6:** Calculation of penalty points for ESA scores.

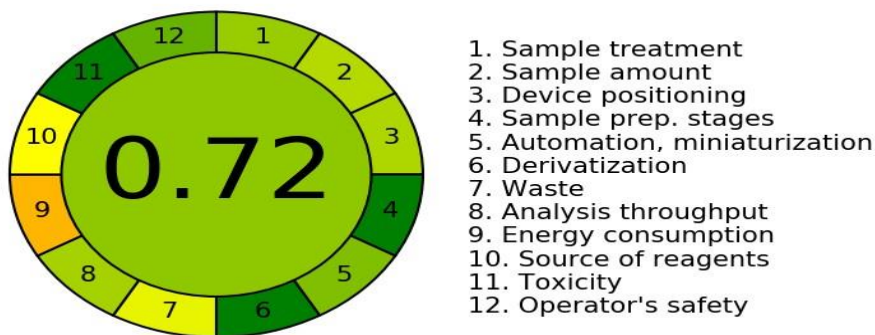
	Analytical Eco-scale	Penalty points
<b>Reagents</b>	HCl	4
	NaOH	2
	H <sub>2</sub> O	0
	Ethanol	4
	FeCl <sub>3</sub>	4
	CoCl <sub>2</sub> .6H <sub>2</sub> O	4
	Phosphoric acid	2
	<b>Instruments</b>	Energy for instrument $\leq 1.5$ KWh/sample
Occupational hazard		0
FESEM		1
Waste (1-10) mL		3
<b>Total penalty points</b>		<b>25</b>
	<b>Eco-Scale total score</b>	<b>75</b>

### AGREE Tool

Based on a company's sustainability level, AGREE evaluates its ecological footprint. The technique is established following the 12 principles of GAC as a guide. As shown in Figure 12a, the 12 principles of Green Analytical Chemistry (GAC) assess how the AGREE instrument affects the environment. Based on the AGREE pictograms, Figure 12a shows different degrees of environmental sustainability with score of 0.72.

**Figure 12:** The assessment of the environmental sustainability of the proposed technique using two pictograms: (a) AGREE, and (b) AGREEprep.

**(a) AGREE**



**(b) AGREEprep tool**

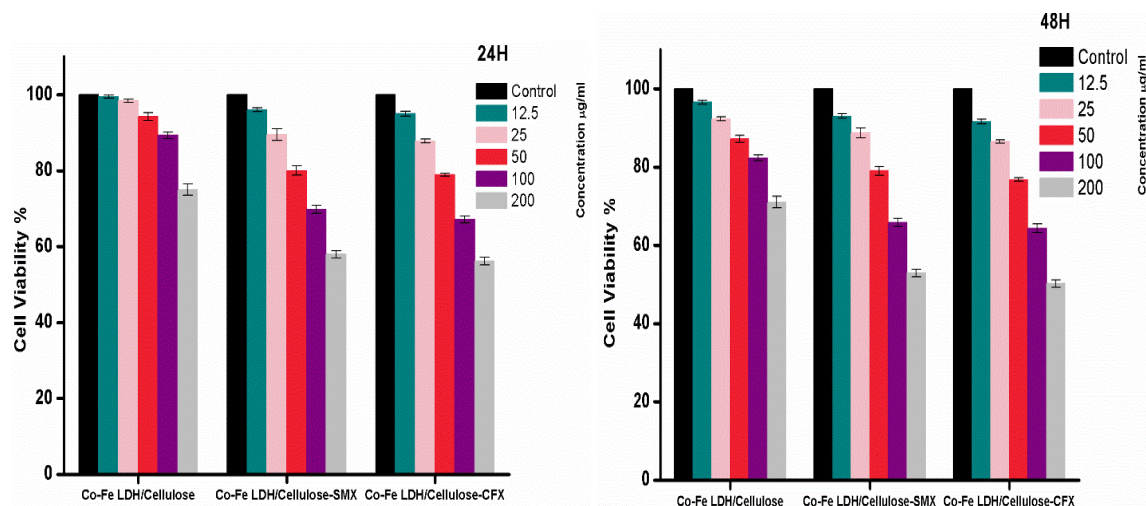


**In vitro Cytotoxicity of Co-Fe LDH/Cellulose, Co-Fe LDH/Cellulose-SMX, and Co-Fe LDH/Cellulose-CFX against Vero cells**

The MTT assay was used to evaluate the potential cytotoxicity of on Vero normal kidney cells. This cell line was treated with increasing concentrations of Co-Fe LDH/Cellulose, Co-Fe LDH/Cellulose-SMX, and Co-Fe LDH/Cellulose-CFX – 12.5, 25, 50 ,100 and 200 µg/ml and incubated for either 24 or 48 hours before assessing cell viability using the MTT assay. As Shown in figure 13, Cells treated with just the diluent served as the control. Co-Fe LDH/Cellulose, Co-Fe LDH/Cellulose-SMX, and Co-Fe LDH/Cellulose-CFX treatments of vero cells for 24 h at 200 µg/ml resulted in 75%,57.9% and 56.2%, respectively cell viability compared to 71%, 52.9% and 50.2% respectively at 48h at the same concentration. These results indicate that LDHs concentrations up to 200 µg/ml did not significantly impact the viability of Vero cell lines following 24- and 48-hour exposures. This suggests LDHs elicited minimal

cytotoxic effects on this cell under the tested conditions. This demonstrates the potential to utilize these LDH-cellulose composites as cytocompatible biomaterials for water treatment applications. The lack of cytotoxic effects validates their usefulness for technologies like antibiotics Residues removal from water where biological compatibility is essential.

**Figure 13:** MTT assay of vero cells with Co-Fe LDH/Cellulose, Co-Fe LDH/Cellulose-SMX, and Co-Fe LDH/Cellulose-CFX at different concentrations for 24 and 48h.



## Conclusions

The cellulose-based LDH has been shown to effectively remove antibiotic residues that pose a direct threat to aquatic ecosystems. Its uniform mesoporous structure and large surface area enhance its ability to remove SMX and CFX from water. The maximum removal efficiency occurs at pH 5 with a 0.1 g dose of adsorbent. The adsorption process was characterized using FTIR, XRD, and FESEM. Six non-linear equilibrium isotherm models were used to fit the experimental data, with a maximum adsorption capacity ( $q_{max}$ ) of 272.13 mg/g for SMX and 208.00 mg/g for CFX. Green chemistry metrics effectively evaluate chemical processes to identify those that adhere to green chemistry principles. The suitability of proposed analytical methods can be confidently evaluated through robust assessment tools such as AGREE, AGREEprep, and ESA. By leveraging these metrics, one can understand the environmental impact of chemical processes and confidently make informed, sustainable decisions. The incorporation of LDH into the cellulose increased the biocompatibility of the LDH nanocomposites.

## Statements and Declarations

### Funding

The authors acknowledge Princess Nourah bint Abdulrahman University Researchers Supporting Project number (PNURSP2024R400), Princess Nourah bint Abdulrahman University, Riyadh, Saudi Arabia.

## Competing Interests

None of the authors have a conflict of interest to disclose

## Data Availability

The datasets used and/or analyzed during the current study available from the corresponding author on reasonable request.

## Ethics Approval and Consent to Participate

Not Applicable as the study not applied on human or animal's study. The article does not include any studies on human participants or animals conducted by any of the authors.

Consent for publication

The authors confirm:

- That the work described has not been published before
- That it is not under consideration for publication elsewhere
- That its publication has been approved by all co-authors

## References

1. Gworek B, Kijeńska M, Wrzosek J, Graniewska M (2021) Pharmaceuticals in the soil and plant environment: a review. *Water, Air, & Soil Pollution* 232: 1-17.
2. Kümmerer K (2009) Antibiotics in the aquatic environment—a review—part I. *Chemosphere* 75: 417-434.
3. Scaria J, Anupama KV, Nidheesh PV (2021) Tetracyclines in the environment: An overview on the occurrence, fate, toxicity, detection, removal methods, and sludge management. *Science of The Total Environment* 771: 145291.
4. Felis E, et al. (2020) Antimicrobial pharmaceuticals in the aquatic environment—occurrence and environmental implications. *European Journal of Pharmacology* 866: 172813.
5. Fowotade A, et al. (2020) Point Prevalence Survey of Antimicrobial Prescribing in a Nigerian Hospital: Findings and Implications on Antimicrobial Resistance. *West African journal of medicine* 37: 216-220.
6. Bourdat-Deschamps M, et al. (2017) Fate and impacts of pharmaceuticals and personal care products after repeated applications of organic waste products in long-term field experiments. *Science of the Total Environment* 607: 271-280.
7. García-Galán MJ, Silvia Díaz-Cruz M, Barceló D, Barceló D (2009) Combining chemical analysis and ecotoxicity to determine environmental exposure and to assess risk from sulfonamides. *TrAC Trends in Analytical Chemistry* 28: 804-819.

8. Elham Sadat Behineh, Ali Reza Solaimany Nazar, Mehrdad Farhadian, H. R. K.-A (2024) Embedded ZnO nanorod array/TiO<sub>2</sub>/GO coated optical fiber in a photocatalytic microreactor for Cefixime degradation: Diffused or focused light sources effect. *Journal of Industrial and Engineering Chemistry*.
9. G Harini, Mohammad K Okla, Mostafa A Abdel-maksoud, B Janani, Ibrahim A Alaraidh, et al. (2024) Effective photodegradation of cefixime and carvedilol mediated by visibly active MoO<sub>3</sub>/CoMn<sub>2</sub>O<sub>4</sub>/Cu<sub>2</sub>BaSn<sub>4</sub> photocatalytic system: An insight on photocatalytic mechanism, degradation pathway and by-product toxicity analysis. *Journal of Industrial and Engineering Chemistry*.
10. Binh VN, Dang N, Anh NTK, Ky LX, Thai PK, et al. (2018) Antibiotics in the aquatic environment of Vietnam: Sources, concentrations, risk and control strategy. *Chemosphere* 197: 438-450.
11. Baran W, Adamek E, Ziemiańska J, Sobczak A (2011) Effects of the presence of sulfonamides in the environment and their influence on human health. *Journal of Hazardous Materials* 196: 1-15.
12. García-Galán MJ, González Blanco S, López Roldán R, Díaz-Cruz S, Barceló D, et al. (2012) Ecotoxicity evaluation and removal of sulfonamides and their acetylated metabolites during conventional wastewater treatment. *Science of The Total Environment* 437: 403-412.
13. Grenni P, Ancona V, Barra Caracciolo A (2018) Ecological effects of antibiotics on natural ecosystems: A review. *Microchemical Journal* 136: 25-39.
14. Liu J, et al. (2020) Early exposure to environmental levels of sulfamethoxazole triggers immune and inflammatory response of healthy zebrafish larvae. *Science of The Total Environment* 703: 134724.
15. Prasannamedha G, Kumar PS, Mehala R, Sharumitha TJ, Surendhar D, et al. (2021) Enhanced adsorptive removal of sulfamethoxazole from water using biochar derived from hydrothermal carbonization of sugarcane bagasse. *Journal of Hazardous Materials* 407: 124825.
16. Li Y, et al. (2022) High performance removal of sulfamethoxazole using large specific area of biochar derived from corncob xylose residue. *Biochar* 4: 1-11.
17. Niu Y, et al. (2023) Highly effective removal of sulfamethoxazole by Na<sub>2</sub>CO<sub>3</sub>-modified biochar derived from sorghum straw and sewage sludge. *Environmental Science: Water Research & Technology* 9: 2355-2367.
18. Martín de Vidales MJ, et al. (2012) Removal of sulfamethoxazole from waters and wastewaters by conductive-diamond electrochemical oxidation. *Journal of Chemical Technology and Biotechnology* 87: 1441-1449.
19. Mostafa Leili MF, Amit B (2018) Green synthesis of nano-zero-valent iron from Nettle and Thyme leaf extracts and their application for the removal of cephalexin antibiotic from aqueous solutions. *Environmental Technology*.
20. Rasouli K, Alamdari A, Sabbaghi S (2023) Ultrasonic-assisted synthesis of  $\alpha$ -Fe<sub>2</sub>O<sub>3</sub>@TiO<sub>2</sub> photocatalyst: Optimization of effective factors in the fabrication of photocatalyst and removal of non-biodegradable cefixime via response surface methodology-central composite design. *Separation and Purification Technology* 307: 122799.
21. Mirzaei M, Sabbaghi S, Zerafat MM (2018) Photo-catalytic degradation of formaldehyde using nitrogen-doped TiO<sub>2</sub> nano-photocatalyst: Statistical design with response surface methodology (RSM). *Canadian Journal of Chemical Engineering* 96: 2544-2552.
22. Khan MA, et al. (2023) Experimental design by response surface methodology for efficient cefixime uptake from hospital effluents using anion exchange membrane. *Chemosphere* 311: 137103.

23. Nabizad M, Dadvand Koochi A, Erfanipour Z (2022) Removal of Cefixime Using Heterogeneous Fenton Catalysts: Alginate/Magnetite Hydroxyapatite Nanocomposite. *Journal of Water and Environmental Nanotechnology* 7: 14-30.
24. Sereshti H, et al. (2022) Sulfide-Doped Magnetic Carbon Nanotubes Developed as Adsorbent for Uptake of Tetracycline and Cefixime from Wastewater. *Nanomaterials* 12.
25. Emami N, Farhadian M, Solaimany Nazar AR, Tangestaninejad S (2023) Adsorption of cefixime and lamotrigine on HKUST-1/ZIF-8 nanocomposite: isotherms, kinetics models and mechanism. *International Journal of Environmental Science and Technology* 20: 1645-1672.
26. Moradi H, et al. (2023) Removal of chloride ion from drinking water using Ag NPs-Modified bentonite: Characterization and optimization of effective parameters by response surface methodology-central composite design. *Environmental Research* 223: 115484.
27. Nanocomposite S, Chiang W, Mousavi SM (2023) Removal of Cefixime from Wastewater Using a Superb.
28. Jia Jia, Xiao Du, Qiqi Zhang, Enzhou Liu JF (2019) Full length article Z-scheme MgFe<sub>2</sub>O<sub>4</sub>/Bi<sub>2</sub>MoO<sub>6</sub> heterojunction photocatalyst with enhanced visible light photocatalytic activity for malachite green removal. *Applied Surface Science*.
29. Deepak Pathania, Rishu Katwal, Gaurav Sharma, Mu. Naushad, Mohammad Rizwan Khan, et al. (2016) Novel guar gum/Al<sub>2</sub>O<sub>3</sub> nanocomposite as an effective photocatalyst for the degradation of malachite green dye. *International Journal of Biological Macromolecules*.
30. Salah Uddin GM, Saha S, Karmaker S, Saha TK (2021) Adsorption of cefixime trihydrate onto chitosan 10b from aqueous solution: Kinetic, equilibrium and thermodynamic studies. *Cellulose Chemistry and Technology* 55: 771-784.
31. Zadvarzi SB, Amooey AA (2023) Amoxicillin and cefixime simultaneous adsorption by facile synthesized chitosan@polyacrylamide@ZIF-8: isotherm and kinetic study. *Environmental Sciences Europe* 35.
32. Zeng S, Choi YK, Kan E (2021) Iron-activated bermudagrass-derived biochar for adsorption of aqueous sulfamethoxazole: Effects of iron impregnation ratio on biochar properties, adsorption, and regeneration. *Science of the Total Environment* 750: 141691.
33. Cheng G, et al. (2022) Surface imprinted polymer on a metal-organic framework for rapid and highly selective adsorption of sulfamethoxazole in environmental samples. *Journal of Hazardous Materials* 423: 127087.
34. Messaoudi NE. Green synthesis of Ag<sub>2</sub>O nanoparticles using Punica granatum leaf extract for sulfamethoxazole antibiotic adsorption: characterization, experimental study, modeling, and DFT calculation.
35. Kadam AA, et al. (2020) Super-magnetization of pectin from orange-peel biomass for sulfamethoxazole adsorption. *Cellulose* 27: 3301-3318.
36. Trygg J, Yildir E, Kolakovic R, Sandler N, Fardim P (2014) Anionic cellulose beads for drug encapsulation and release. *Cellulose* 21: 1945-1955.
37. Mandal S, Mayadevi S (2008) Cellulose supported layered double hydroxides for the adsorption of fluoride from aqueous solution. *Chemosphere* 72: 995-998.
38. Imeson AP (2012) Thickening and Gelling Agents for Food. Springer Science & Business Media.
39. Liu S, Tao D, Zhang L (2012) Cellulose scaffold: A green template for the controlling synthesis of magnetic inorganic nanoparticles. *Powder technology* 217: 502-509.

40. Liu Y, Goebel J, Yin Y (2013) Themed issue: Chemistry of functional nanomaterials. *Chem. Soc. Rev* 42: 2610-2653.
41. Anastas P, Eghbali N (2010) Green Chemistry: Principles and Practice. *Chemical Society Reviews* 39: 301-312.
42. Gałuszka A, Migaszewski Z, Namieśnik J (2013) The 12 principles of green analytical chemistry and the SIGNIFICANCE mnemonic of green analytical practices. *TrAC - Trends in Analytical Chemistry* 50: 78-84.
43. Mahgoub S, et al. (2023) Analytical assessment of a novel RP-HPLC method for the concurrent quantification of selected pharmaceutical drugs levodopa and carbidopa using eight greenness metrics comparing to the lean six sigma approach. *Sustainable Chemistry and Pharmacy* 36: 101291.
44. Tahani YA Alanazi a, Manal A Almalki b, Mahmoud A, Mohamed c, et al. (2023) Five greenness assessments of novel RP-UPLC and MCR methods for concurrent determination of selected pharmaceutical drugs in comparison with the lean Six Sigma approach. *Microchemical Journal* 194.
45. Gałuszka A, Migaszewski ZM, Konieczka P, Namieśnik J (2012) Analytical Eco-Scale for assessing the greenness of analytical procedures. *TrAC - Trends in Analytical Chemistry* 37: 61-72.
46. Kowtharapu LP, Katari NK, Sandoval CA, Rekulapally VK, Jonnalagadda SB (2022) Green Chromatographic Method for Determination of Active Pharmaceutical Ingredient, Preservative, and Antioxidant in an Injectable Formulation: Robustness by Design Expert. *ACS Omega* 7: 34098-34108.
47. Pena-Pereira F, Wojnowski W, Tobiszewski M (2020) AGREE - Analytical GREENness Metric Approach and Software. *Analytical Chemistry* 92: 10076-10082.
48. Krishankant, et al. (2023) A 3D-hierarchical flower like architecture of anion induced layered double hydroxides for competing anodic reactions. *Energy Advances* 2: 1674-1684.
49. Nalintip Imchalee, Ratthapong Meesupthong, Selorm Torgbo PS. Cellulose nanocrystals as sustainable material for enhanced painting efficiency of watercolor paint. *Surfaces and Interfaces*.
50. Fang Luo ZC, Mallavarapu Megharaj RN (2016) Simultaneous removal of trichloroethylene and hexavalent chromium by green synthesized agarose-Fe nanoparticles hydrogel. *Chemical Engineering Journal*.
51. Yang C, et al. (2020) Highly efficient removal of amoxicillin from water by Mg-Al layered double hydroxide/cellulose nanocomposite beads synthesized through in-situ coprecipitation method. *International Journal of Biological Macromolecules* 149: 93-100.
52. Abo El-Reesh GY, Farghali AA, Taha M, Mahmoud RK (2020) Novel synthesis of Ni/Fe layered double hydroxides using urea and glycerol and their enhanced adsorption behavior for Cr(VI) removal. *Scientific Reports* 10: 1-20.
53. Chen Y, Cui J, Liang Y, Chen X, Li Y, et al. (2021) Synthesis of magnetic carboxymethyl cellulose/graphene oxide nanocomposites for adsorption of copper from aqueous solution. *International Journal of Energy Research* 45: 3988-3998.
54. Yang C, Yuan J, Guo Y, Luo X (2021) In situ nano-assembly of Mg/Al LDH embedded on phosphorylated cellulose microspheres for tetracycline hydrochloride removal. *Cellulose* 28: 301-316.

55. Xiaogang Luo, Hao Zhang, Zhenni Cao, Ning Cai, Yanan Xue, et al. (2016) A simple route to develop transparent doxorubicin-loaded nanodiamonds/cellulose nanocomposite membranes as potential wound dressings. *Carbohydrate Polymers*.
56. Pooresmaeil M, Behzadi Nia SNHG (2019) encapsulation of LDH(Zn/Al)-5-Fu with carboxymethyl cellulose biopolymer; new nanovehicle for oral colorectal cancer treatment. *Int J Biol Macromol*.
57. Hussein OG, Abdou K, Moselhy WA, Mahmoud R (2023) Ternary layered double hydroxide/3-amino-1H-1,2,4-triazole for high-efficiency removal of copper metal ions. The experimental, possible mechanism, sustainable use of waste, and safety study. *Applied Clay Science* 231: 106724.
58. Boukmouche N, Azzouz N, Bouchama L, Chopart JP, Bouznit Y, et al. (2014) Activated carbon derived from marine *Posidonia Oceanica* for electric energy storage. *Arabian Journal of Chemistry* 7: 347-354.
59. Emami N, Farhadian M, Solaimany Nazar AR, Tangestaninejad S (2023) Adsorption of cefixime and lamotrigine on HKUST-1/ZIF-8 nanocomposite: isotherms, kinetics models and mechanism. *International Journal of Environmental Science and Technology* 20: 1645-1672.
60. Zhang CL, Cui SJ (2017) Thermodynamics of sulfamethoxazole dissolution in organic solvents at 293.15–323.15 K. *Russian Journal of Physical Chemistry A* 91: 1051-1055.
61. Sanli N, Sanli S, Sızır U, Gumustas M, Ozkan SA, et al. (2011) Determination of pK<sub>a</sub> values of cefdinir and cefixime by LC and spectrophotometric methods and their analysis in pharmaceutical dosage forms. *Chromatographia* 73: 1171-1176.
62. Bidhendi ME, et al. (2020) Nano-size biomass derived from pomegranate peel for enhanced removal of cefixime antibiotic from aqueous media: Kinetic, equilibrium and thermodynamic study. *International Journal of Environmental Research and Public Health* 17: 1-15.
63. Al-Gorair AS (2019) Treatment of wastewater from cationic dye using eco-friendly nanocomposite: Characterization, adsorption and kinetic studies. *Egyptian Journal of Aquatic Research* 45: 25-31.
64. Sun S, Yu E, Hu R, Li Y, Wei Z, et al. (2023) Synthesis and study of poly (phthalic anhydride- $\beta$ -cyclodextrin) for the efficient adsorption of cationic dyes from industrial wastewater. *Chemical Engineering Research and Design* 194.
65. Younes HA, et al. (2019) Computational and experimental studies on the efficient removal of diclofenac from water using ZnFe-layered double hydroxide as an environmentally benign absorbent. *Journal of the Taiwan Institute of Chemical Engineers* 102: 297-311.